Observing Optically Dark States in the Photoswitchable Azobenzene with Resonant Inelastic X-ray Scattering

Zhong Yin,[*,†,‡,¶,∇] Ambar Banerjee,[*,§,∇] Ivan Rajkovic,[¶,‖] Emelie Ertan,[⊥] Annette Pietzsch,[#] Alexander Föhlisch,[*,#,@] Simone Techert,[*,‡,¶,△] and Michael Odelius[*,⊥]

†*International Center for Synchrotron Radiation Innovation Smart, Tohoku University, 980-8572, Sendai, Japan.*

‡*Deutsches Elektronen-Synchrotron DESY, Photon Science,22607 Hamburg, Germany.*

¶*Max Planck Institute for Biophysical Chemistry, Structural Dynamics of (Bio)chemical Systems, 37077 Göttingen, Germany.*

§*Research Institute for Sustainable Energy (RISE), TCG Centres for Research and Education in Science and Technology (TCG-CREST), Kolkata, 700091 India.*

‖*SLAC National Accelerator Laboratory, Menlo Park, California 94025, USA.*

⊥*Department of Physics, Stockholm University, AlbaNova University Center, 10691 Stockholm, Sweden.*

#*Helmholtz Zentrum Berlin, Albert Einstein Str. 15, 12489 Berlin, Germany.*

@*University of Potsdam, Karl-Liebknecht-Str. 24-25, 14476 Potsdam, Germany.*

△*University of Göttingen, Institute for X-ray Physics, 37077 Göttingen, Germany.*

∇*contributed equally*

E-mail: yinz@tohoku.ac.jp; ambar.banerjee@tcgcrest.org; alexander.foehlisch@helmholtz-berlin.de; simone.techert@desy.de; odelius@fysik.su.se

Abstract

The trans-cis isomerization in azobenzene is a reversible reaction that has strong application potential ranging from photo-stimulating molecular motors to molecular electronics. Though azobenzene has been intensively and thoroughly investigated in optical spectroscopy, the $S_0 \rightarrow S_1$ transition is symmetry forbidden. Here, we report on measurements of resonant inelastic X-ray scattering (RIXS) at the nitrogen K-edge of the trans- and cis-forms of azobenzene dissolved in ethanol. In RIXS, we observe isomer-specific spectral features, which contain a distinct signature of the S_1 state and further information on the electronic properties of the isomers of azobenzene. For the cis-isomer an additional peak arises, revealing a transition suppressed in the trans-conformation due to different orbital hybridization, thereby giving distinct spectral fingerprints to the trans- and cis-isomers of azobenzene in RIXS, containing information about valence excitations and their nitrogen character.

Introduction

Photoisomerization is a fundamental process in photochemistry,[1–3] in which photoabsoption triggers the molecule to change its structural conformation, without alterations of the connectivity within the molecules. Generally, photoinduced isomerization is of utmost importance in biochemistry. It is involved in key reactions in the process of vision and triggers the motion of biological entities towards light.[4,5] Hence, systems undergoing photoisomerization are often implemented in biochemical applications to remotely control cell receptors and membran channels.[5–7] Furthermore, they are being assessed or use in the growing fields of organic electronics,[8,9] molecular machines and batteries.[10,11]

Trans- and cis-azobenzene (AB) are conformational isomers consisting of two phenyl rings bridged by an N=N double bond moiety, representing the simplest azo-aromatic system and a model system for photo-induced isomerization processes. The reversible trans (E) - cis (Z) isomerization process can be triggered upon photo-irradiation,[12–15] see Figure 1(a). Fig-

ure 1(b) shows the ultraviolet-visible (UV-vis) spectra of trans- and cis-azobenzene. The weak peak at ($\sim$440 nm) corresponds to the S_1 state, with a low intensity, associated with a symmetry forbidden n$\rightarrow \pi^*$ transition, while the strong peak at $\sim$320 nm corresponds to the S_2 state associated with a symmetry allowed $\pi \rightarrow \pi^*$ transition, see Figure 1(b). The cis-AB sample was prepared from a solution of trans-AB by UV-radiation. The photoisomerization of azobenzene is the simplest form of an externally triggered molecular motion. The different isomerization processes can be divided into two classes, where one involves a weakening of the N=N double bond through a torsional motion and the other proceeds though an in-plane inversion of one of the nitrogen centers.[1] While the S_2 state can be directly populated in a UV excitation, the S_1 is optically "dark". Optically dark states play a vital role in the energy dissipation of bio-molecules after photo-absorption. Excitation into bright states can trigger excited state dynamics involving transient dark states before reaching the ground state. They are subject to intense research, in particular, due to their relevance for the photo-stability of DNA bases.[16] From a more fundamental perspective, optically dark states are populated through photo-induced coupled nuclear and electronic dynamics, which typically is very challenging to measure and simulate.[17–19] Excited state dynamics pathways in azobenzene has been studied with vibrational Raman spectroscopy[20] transient absorption spectroscopy,[21] and modeled through non-adiabatic simulations.[22] Substituents and confinement strong influences the excited state dynamics.[23] There have been theoretical demonstrations to monitor conical intersection dynamics with ultrafast electron diffraction.[24]

In this work, we investigate trans- and cis-azobenzene with resonant inelastic X-ray scattering (RIXS).[25,26] In RIXS, the excitation energy is tuned around a resonance in an X-ray absorption (XA) edge of a particular element, thereby initiating an electronic scattering process involving electrons from the corresponding core level and the valence band. Inelastic scattering against the intermediate core-excited state gives rise to a manifold of elementary low-energy excitations. The reoccupation of the core-hole by an electron from the valence

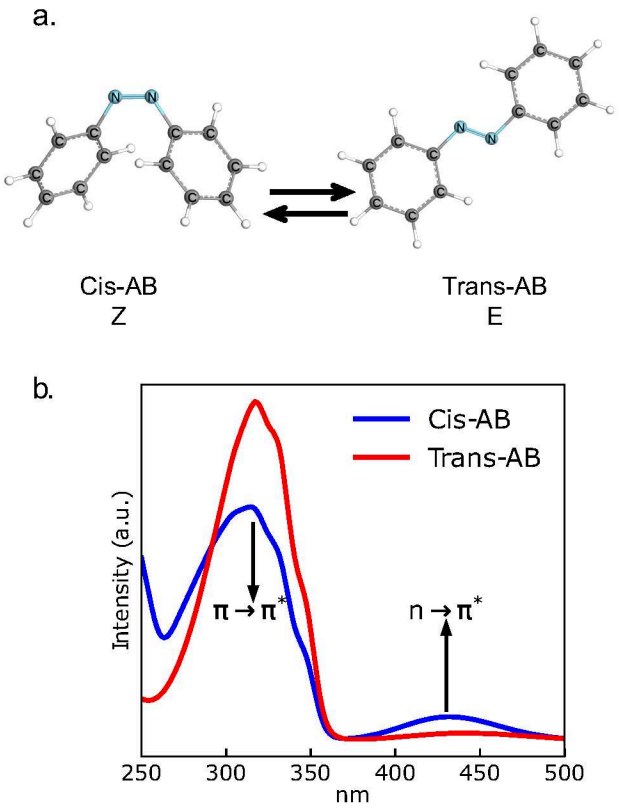

Figure 1: Trans-cis isomerization and photochemistry of Azobenzene. a. The molecular structures of the trans- and cis-isomers of azobenzene. b. The UV-vis spectra of the isomers of azobenzene in ethanol share a strong $\pi \rightarrow \pi^*$ transition associated with the bright S_2 state. The cis-isomer poses a weak peak around 440 nm, which is absent in the trans-isomer. This weak/absent n$\rightarrow \pi^*$ transition corresponds to the dark S_1 state.

band under emission of an X-ray photon occurs on the few femtosecond time-scale.[27] The sensitivity to low energy excitations in electronic, vibrational, phononic and magnetic degrees for freedom has lead to fundamental discoveries in the fields of correlated material, atomic and molecular system and liquids.[25–28] However, the application of soft X-ray spectroscopy to chemistry has progressed in parallel with the development of modern light sources, such as synchrotrons, free-electron lasers, and table-top water-window sources, owing to the challenges of sample delivery, as most chemical processes occur in the liquid phase and require dedicated experimental setups.[29–36] Nevertheless, RIXS as a probe of chemical processes in their natural environment has a strong potential because chemical bonding properties are

reflected in the local electronic configuration which can be monitored with site selectivity by probing different X-ray resonances. Conventional techniques are spectroscopic methods in the optical to the far infrared regimes, containing vibrations, rotational and low valence excitations. A common principle in RIXS and optical spectroscopy is the importance of selection rules for the electronic transitions. However, the underlying processes are different and transitions that are forbidden for direct excitations in the optical regime, *i.e.* the n$\rightarrow \pi^*$ transition on azobenzene, can give strong features in RIXS. Also, while the final state is the same as in the optical regime, RIXS involves an intermediate core-excited state and inherent relaxation processes. Having element selectivity and chemical sensitivity, RIXS is an important complement to optical spectroscopy and can be utilized to investigate optically dark states of chromophores in solution.

X-ray absorption spectroscopy (XAS) has been successfully applied, both experimentally and theoretically, to the investigation of azobenzene in the gas phase[37–40] and has become a widely used probe of azobenzene-based monolayers on surfaces.[41,42] More recently, self-referencing XAS of 4-aminoazobenzene has also been demonstrated at a free-electron laser.[43] However, gas-phase studies omit solvation interactions, and the FEL study prioritized methodological validation without an isomer-resolved comparison.

Here, the first measurements of X-ray absorption (XA) and RIXS spectra of trans- and cis-azobenzene in ethanol solution on the nitrogen K-edge are presented and we identify spectroscopic signatures unique to individual isomers. In particular, we show polarization-dependent RIXS measurements to investigate the relative orientation of the molecular orbitals (MOs). The distinct spectral fingerprints identified in this work can be utilized in future studies of the photochemistry of azobenzene. Spectral simulations were performed neglecting vibrational excitations,[27] and electronically excited states associated with the relevant spectral peaks were identified and discussed within the framework of time-dependent density functional theory (TDDFT).

Methods

Experimental Method

Trans-azobenzene solutions (200 mM) were prepared from commercially available compounds from Sigma Aldrich with 98% purity and dissolved in ethanol of highest purity, followed by filtering. The cis-AB sample was prepared from a trans-AB solution by UV radiation with a centered wavelength around 365 nm. Since at UV wavelength the absorption yield is much higher for trans- than cis-azobenzene, the backconversion due to UV absorption is negligible. During the UV irradiation, the sample was kept protected from the ambient light and cooled to minimize thermal back isomerization. Optical measurements were carried out with a Cary 5E from Varian UV-Vis spectrophotometer to confirm the creation of the cis-AB isomer. Figure 1(b) shows the optical spectrum of diluted trans-AB before and after UV radiation. The typical characteristic spectrum in the UV range is observed confirming the existence of trans- and cis-azobenzene.[1] The UV-vis spectrum shows the S_2 band at $\sim$440 nm ($\sim$2.8 eV) and S_1 at $\sim$320 nm ($\sim$3.9 eV).

The RIXS experiments were carried out at the U41 PGM and U52 SGM using the FlexRIXS setup at HZB.[29] The spectrometer resolution was set to 0.3-0.4 eV and the beamline bandwidth was around 0.2 eV. The elastic peaks were used for energy calibration. The X-ray absorption measurement at P04 at PETRA III with the ChemRIXS endstation was performed in total fluorescence yield mode with a commercial photodiode.[30] In all experiments a nozzle with an orifice of $\sim$25 μm was utilized. The total fluoresence data were normalized to the peak maximum of the lowest π^* resonance. The experimental and theoretical RIXS spectra were normalized to the elastic peak. In the presentation of the polarization results, the RIXS spectra were normalized to the area excluding the elastic peak and vibrational progressions, corresponding to the range from approximately 1.85 eV to 20 eV for trans-AB, and from around 2.6 eV to 20 eV for cis-AB on the energy loss scale.

Theoretical Method

Two different solvation models were employed for the computation of nitrogen K-edge XA and RIXS spectra of trans- and cis-isomers of azobenzene. The models differ in the way we describe the solvation of azobenzene in ethanol. In a simple model, the azobenzene molecule was placed within an implicit solvation model, the conductor-like polarizable continuum (CPCM) model, having ethanol as solvent,[44] which we denote as TDDFT/CPCM, when referring to TDDFT computations. In a more advanced model, we included explicit ethanol molecules hydrogen bonded to the two nitriogen atoms of azobenzene, thereby accounting for a limited explicit solvation model and also surrounded by the implicit solvation model. This model is denoted TDDFT/HB+CPCM.

The structures of trans- and cis-AB in the two models were optimized with M06-2X density functional[45] and def2-TZVP basis sets.[46] The M06-2X functional is known to give superior performance in geometry optimization especially for hydrogen bonded systems.[47] The optimized structures were checked for the absence of imaginary frequencies. All optimization were carried out with the Gaussian16 quantum chemistry package.[48] With these optimized geometries, nitrogen K-edge XA and RIXS spectra were computed using the restricted subspace TDDFT[49] method in the ORCA-4.2.0 quantum chemistry suite.[50] For restricted subspace TDDFT computations of XAS and RIXS spectra we employed the CAM-B3LYP[51] functional and def2-TZVP basis set.[46] The CAM-B3LYP functional is known to estimate the absorption spectra of Azo-benzene accurately[52] and hence was employed to simulate XAS and RIXS. The restricted subspace TDDFT method was employed to reach both the core-excited states and valence-excited states while solving for only a limited number of roots. In the restricted subspace TDDFT calculations, the excitation space comprised of HOMO to HOMO-20 and two N1s core-orbitals included as occupied orbitals and LUMO to LUMO+20 as unoccpied orbital. This orbital subspace is employed for both the models, TDDFT/CPCM and TDDFT/HB+CPCM. Then all excitation was solved in this orbital subspace, which included 420 valence-excited states and 40 core-excited states. Transition

dipole moments between ground, valence-excited state and core-excited states were also computed using Multiwfn program package.[53]

The transition dipole moments between ground, valence-excited states and core-excited states were extracted from subspace TDDFT computations and used for simulating the polarization dependent RIXS using our own code. The code is based on the theory developed by Gel'mukhanov et al.[54] The theoretical results were convoluted with a Gaussian broadening of 0.35 eV full-width at half-maximum to approximately account for experimental energy resolution, core-excited state life-time, and vibrational broadening. For both models, the simulated XA spectra were shifted so that the pre-edge peak for trans-azobenzene align with the experimental value for an easier comparison of relative energy shifts of the two isomers.

Results and Discussion

Figure 2 shows the pre-edge ($1s \rightarrow \pi^*$) region of the experimental nitrogen K-edge X-ray absorption data of the isomers of azobenzene along with the comparison to simulated XA spectra derived from TDDFT calculations on the two solvation models. The experimental X-ray absorption (XA) spectra show a peak at 398.8 eV for the trans-isomer and at 398.9 eV for the cis-isomer. The blue shift of ∼0.1 eV is smaller than the shift of 0.45 eV reported for isomarization in tetra-tert-butyl-azobenzene monolayers on a gold substrate.[41] In the middle and bottom tiers, the spectra of the calculated isomers for both models, TDDFT/HB+CPCM with hydrogen bonding (HB) and TDDFT/CPCM without HB, are shown. For the simulated spectra, we find that the experimental energy shift for peaks is best captured in the TDDFT/HB+CPCM model and is overestimated by 0.15 eV in the TDDFT/CPCM model, where hydrogen bonding is not explicitly accounted for. This is also reflected in the fact that indeed for azobenzene on a gold surface ,[41] where no hydrogen bonding exists among other effects, the energy shift is more aligned with the spectral shift simulated using the TDDFT/CPCM model.

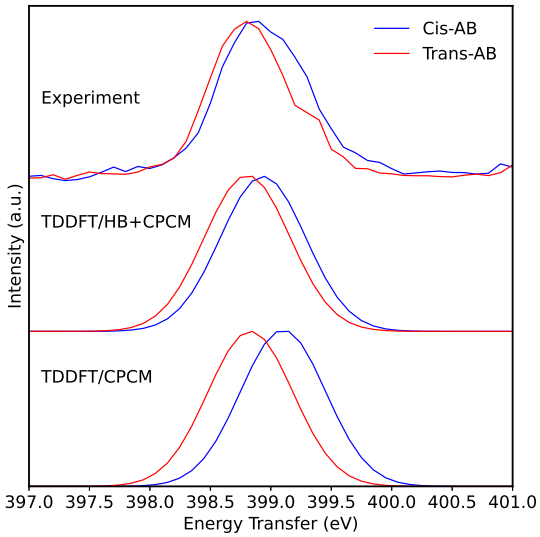

Figure 2: X-ray absorption spectra of trans-(red) and cis- (blue) azobenzene at the nitrogen K-edge. Simulated XA spectra from the two different solvation models are evaluated against the experimental spectra. The spectra are normalized to equal peak height. The calculated spectra align to experiment for the trans-isomer.

Accurate modeling of RIXS requires a faithful representation of ground and valence-excited states as well as intermediate core-excited states in the RIXS process.[55] For this purpose, we employed TDDFT and the restricted subspace method.[49] The relevant molecular orbitals, needed to simulate the RIXS spectra, are shown in Figure 3(a) and (b), for both the models at their respective optimized geometries.

In Figure 4(a), we present the experimental and simulated RIXS of trans- and cis-azobenzene at the nitrogen ($1s \rightarrow \pi^*$) resonance. The experimental RIXS spectra contains three peaks with distinct energy transfers below 5 eV. The elastic peak at 0 eV energy transfer, associated with scattering back to the electronic ground state, exhibits an asymmetry associated with vibrational excitations. The unresolved vibrational progression of the elastic line is due to ultrafast nuclear dynamics in the RIXS process.[27] At higher energy resolution than in the current experiment, the vibrational progression could be used to investigate the shape of the ground state potential energy surface.[56,57] In Figure 4(a), the experimental and simulated RIXS spectra for both isomers are normalized with respect to this elastic line.

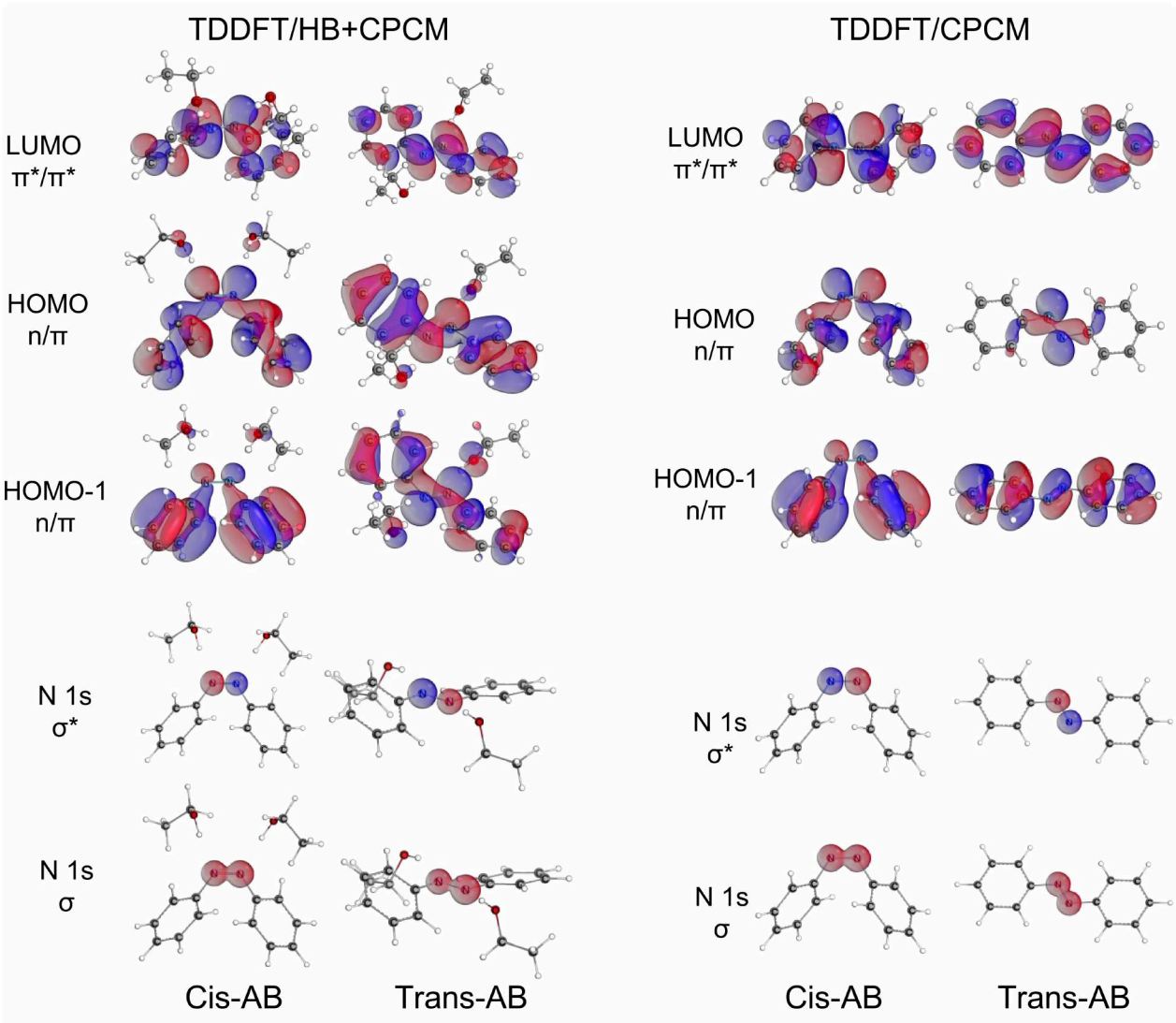

Figure 3: a. Molecular orbitals involved in the low energy loss features in nitrogen K-edge RIXS of trans- and cis-isomers of azobenzene in the TDDFT/HB+CPCM model. b. Corresponding orbitals in the TDDFT/CPCM model. The molecular orbitals are plotted with IboView at 80% viewing threshold.

In the experimental spectra, we observe a distinct peak around 3.1 eV for both isomers of azobenzene, having higher intensity for the trans-isomer than for the cis-isomer. The simulated spectra in the TDDFT/HB+CPCM model also reproduce this peak at 3.2 eV for the trans-isomer and at 3.1 eV for the cis-isomer, with a more intense peak in the trans-isomer than in the cis-isomer.

In a simplistic one-electron picture of RIXS, a core-electron is first excited to an unoc-

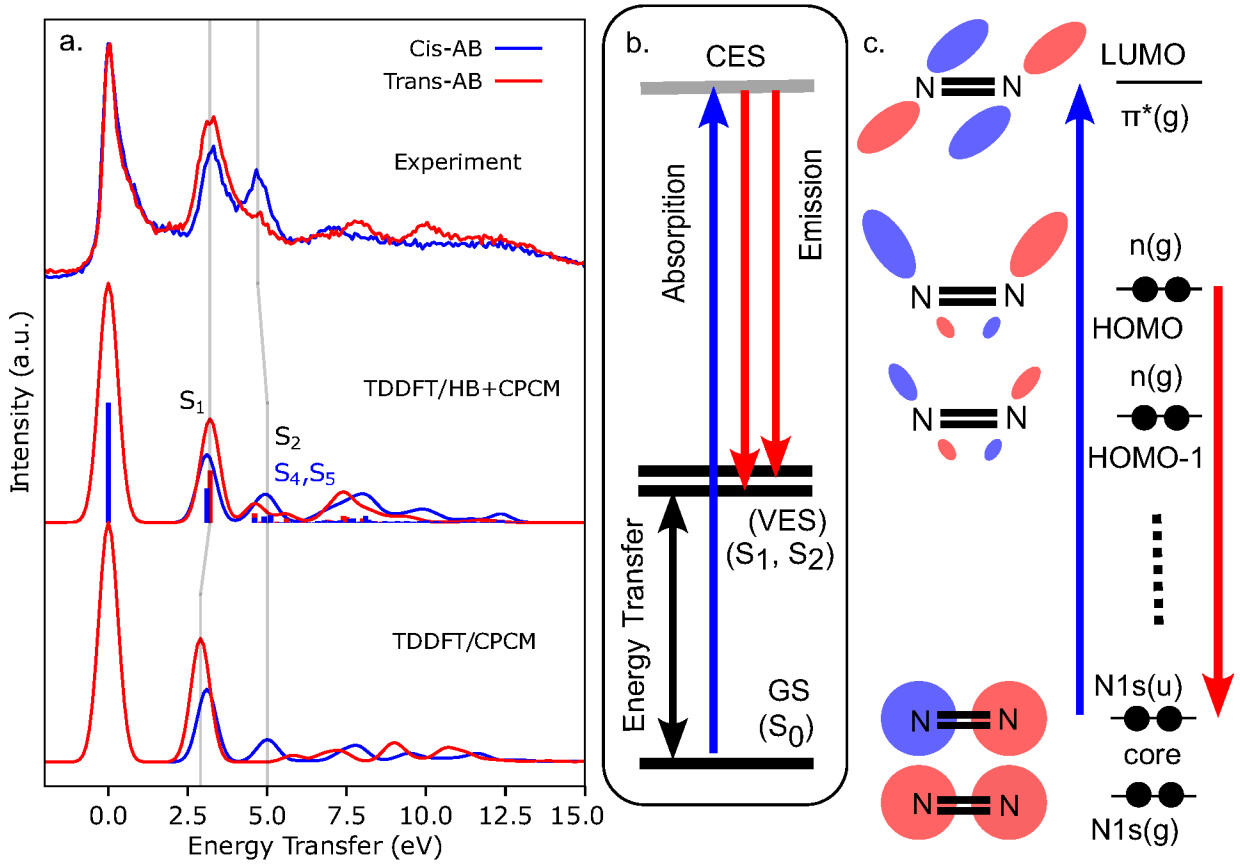

Figure 4: Nitrogen K-edge RIXS for trans- and cis-AB a. Experimental and simulated RIXS spectra for scattering against the XA pre-edge shown in Figure 2. The excitation energy was set at around 399.4 eV. b. The RIXS process involving ground S_0 and valence-excited states (VES) $S_{1,2}$ and the lowest core-excited states (CES) in the electronic state picture. c. The RIXS process in the one-electron picture, including schematic diagram for character of the orbitals involved in the lowest valence-excited states and the core-excited state.

cupied orbital, *e.g.* LUMO, followed by radiative emission from the decay of an electron from the same orbital or from another occupied valence orbital into the core-hole, see Figure 4(c). Therefore, the final state in RIXS can be a valence-excited state that also could be reached in optical absorption, see Figure 4(b,c). The first inelastic peak corresponds to the S_1 valence-excited final state which involves the HOMO $\rightarrow$ LUMO transition. The HOMO of azobenzene comprises of the anti-bonding combination of the two N lone pair orbitals, see Figure 4(d). The planar trans-isomer is inversion symmetric and thus has higher symmetry than the cis-isomer with its turned and flipped benzene rings. This means that in the trans-isomer, assuming a negligible symmetry-breaking of of the solvent, symmetry selection rules for photo-excitation are strictly followed and with both HOMO and LUMO of trans-AB having gerade symmetry, the optical transition is strictly forbidden. In the case of cis-AB with its reduced symmetry, selection rules are weakened and transitions that are symmetry forbidden in trans-AB, such as S_1, can be observed in the UV-vis spectrum.

For local excitation at the N atoms, the symmetry properties are inherited from the local symmetry around the N atoms since the valence electronic states that stretch across the molecule are imaged onto the local N-sites. Since the XA spectroscopy and RIXS are element specific probes, the local symmetry around specific elements plays an important role. The LUMO of azobenzene is the N=N π^* orbital, which in the trans-isomer has gerade symmetry, see Figure 4(d). The S_1 state has very low intensity in the UV-vis spectra corresponding to the n$\rightarrow$ π^* transition. Since, the HOMO and LUMO of the trans-isomer have gerade inversion symmetry, the optical transition is strictly forbidden. The two N 1s orbitals can combine to give a gerade and an ungerade orbital, see Figure 4(d). The RIXS process at the resonance involves a symmetry allowed excitation from core-orbital of ungerade symmetry into the LUMO, creating a core-hole, and subsequently an electron from the HOMO decays to fill the core-hole in another symmetry allowed transition.

The S_1 state for the trans-isomer corresponds to a optically symmetry forbidden n$\rightarrow$ π^* transition, owing to the C_{2h} symmetry of trans-AB. It has a very weak intensity in the UV-vis

spectrum in Figure 1(b). However for the cis-isomer, lacking the C_{2h} symmetry, this peak is somewhat more intense than for the trans-isomer. Since in RIXS the process involves three levels, both in the electronic state and one-electron pictures (see Figure 4(b,c)), instead of a two-level process as in UV-vis spectra, the S_1 state, particularly for the trans-isomer, can be targeted. Thus, we establish that the optically dark S_1 state can be probed in RIXS.[58] The energy transfers corresponding to the first inelastic peak in the experimental RIXS spectra are very similar for the two isomers. This is also reproduced in both models, though the TDDFT/HB+CPCM model predicts a slight red shift and TDDFT/CPCM predicts a slight blue shift of the S_1 peak for the cis-isomer, see Figure 4(a).

As seen from the experimental spectra in Figure 4(a), there is a distinct peak at 4.7 eV in the cis-isomer. The trans-isomer lacks a distinct peak, though a shoulder at the corresponding position can be identified. The TDDFT/HB+CPCM model reproduces the distinct peak for the cis-isomer, and a lower intensity peak for the trans-isomer. The shoulder of the first inelastic peak for the trans-isomer as observed in the experimental spectra, can be associated with the low intensity peak in simulated spectra of the trans-isomer or may be due to the vibrational progression . We found that several valence-excited states (S_2, S_4, and S_5) contribute to the formation of the inelastic peak at 4.7 eV in the cis-isomer, though for the trans-isomer we have a major contribution from the S_2 state.

Interestingly in the TDDFT/CPCM model, where explicit hydrogen bonding interaction is missing, the shoulder of the first inelastic scattering peak for the trans-isomer is not reproduced, see Figure 4(a). This demonstrates the necessity for the inclusion of explicit hydrogen bonding models in simulation of RIXS spectrum of such systems. In the one-electron picture, the S_2 and also S_4 and S_5 valence-excited states (for the cis-isomer) correspond to excitations creating a hole in doubly occupied molecular orbitals and putting an electron in the LUMO. These occupied molecular orbitals have an anti-bonding combination of the two nitrogen lone pairs, but with much smaller coefficients and the dominant coefficients corresponding to the π^* orbital of the phenyl moiety. In order to adress the nature of the orbitals, we also

performed polarization dependent RIXS measurements.

The RIXS spectra for vertical and horizontal polarization for two isomers are given in Figure 5(a,b). The spectral difference between vertical and horizontal polarization was also derived, revealing that the first inelastic peak has a small yet clear polarization dependence. It is stronger in the horizontally polarized RIXS spectra than in the vertically polarized RIXS spectra. The polarization dependence is more pronounced for the trans-isomer than for cis. This indicates that the directions of local 2p character of the nitrogen HOMO and LUMO of azobenzene are oriented perpendicular to each other. This is in particular true for the inversion symmetric trans-isomer: In a simplified 2-step RIXS process the selective excitation from N 1s into the LUMO (oriented perpendicular to the molecular backbone) is followed by emission from states oriented along the backbone. The molecular orbitals of the cis-isomer do not show such a clear orientation due to the reduced molecular symmetry and polarization-dependent RIXS can thus reach a larger number of differently oriented molecular orbitals. The polarization dependence being more pronounced for trans-AB compared to cis-AB suggests that the structural orientation of the two benzene rings influences the molecular orbital orientation at the nitrogen atoms.

Conclusions

In this work, we present experimental XA spectra and RIXS data of trans- and cis-azobenzene probed in the liquid phase. Both isomers exhibit a strong XA pre-edge resonance and a distinct first inelastic peak in RIXS. Additionally, an extra peak is observed in the cis-isomer, which is strongly suppressed in the trans-isomer, indicating a lifting of degeneracy after complex change in the electronic structure following structural rearrangement. Theoretical calculations successfully reproduce the major spectral features and trends, further elucidating the origin of our experimental findings. This work demonstrates that RIXS can be used to probe optically dark states in the X-ray regime, providing valuable insights into the excited

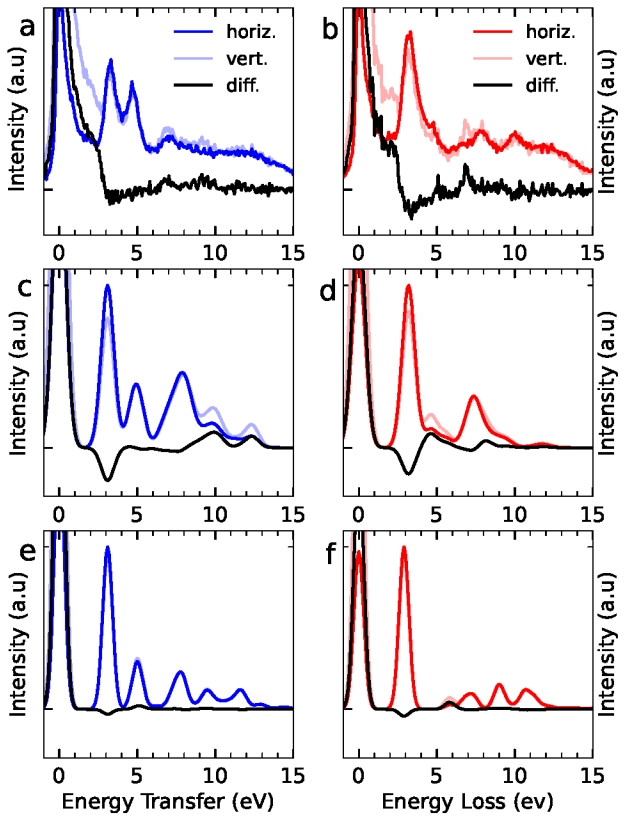

Figure 5: Comparison of experimental spectra (a-b) for vertical and horizontal polarization with theoretical results for the TDDFT/CPCM (c-d) and TDDFT/HB+CPCM (e-f) models of cis- (blue) and trans- (red) azobenzene. In each panel a-f, we persent the vertical (light color), horizontal (dark color), and difference (black) RIXS signal. The area normalization is described in the Methods Section.

state properties of azobenzene. Furthermore, hydrogen bonding is essential for accurately simulating the interaction of azobenzene with ethanol. Overall, the electronic structures of trans- and cis-azobenzene are distinguishable, enabling future studies on the isomerization pathways of azobenzene,[22] an area that cannot be fully addressed with the current static RIXS results.

In light of recent developments in upgraded free-electron laser facilities, such as the European XFEL and LCLS-II, which offer high repetition rates up to the MHz range and high photon energies with tailored properties such as bandwidth and pulse duration, these advancements could help address unresolved questions.[22] Additionally, recent theoretical studies have suggested using ultrafast X-ray or electron diffraction[59] or entangled two optical photons[60] to follow isomerization pathways after optical excitation. Diffraction methods can be used to image structural changes. However, diffraction and two-photon absorption would lack of element specificity, which may lead to strong contributions from the carbon signals of the phenyl rings and solvent molecules, potentially complicating the identification of the isomerization dynamics. Another approach suggests to study coupled vibrational–electronic dynamics as states traverse conical intersections with by time-resolved Auger spectroscopy.[61] In contrast, the current static RIXS results demonstrate the potential of an element-selective approach. This could pave the way for time-resolved RIXS, which would provide deeper insights into the ultrafast isomerization dynamics by selectively probing specific atomic centers. This approach can be combined with the rapidly advancing field of hybrid light–matter, polaritonic, states, which leverages light itself to control molecular photochemistry, circumventing the need for synthetic or environmental modifications.[62]

Conflicts of interest

There are no conflicts to declare.

Author contributions

The experiment was conceived by S.T. and A.F. Experiments were performed by Z.Y., I.R., A.P. and analyzed by Z.Y and I.R. Calculations were performed and analyzed by A.B., E.E., and M.O. The paper was written by Z.Y., A.B., A.P., and M.O. with input from all co-authors. Graphics were prepared by Z.Y. and A.B. S.T, A.F and M.O supervised the project.

Data availability

The datasets generated and analyzed during the current study can be accessed on Zenodo `https://doi.org/10.5281/zenodo.16909283`. Further information is available from the corresponding authors on reasonable request.

Acknowledgement

This project was supported by SFB755 "Nanoscale Photonic Imaging" and SFB 1073 "Atomic Scale Control of Energy Conversion" of the German Science Foundation (DFG), the Advanced Study Group of the Max Planck Society, Deutsches Elektronen-Synchrotron, Helmholtz Zentrum Berlin. S.T. is grateful to the Funds of the Chemical Industry. We thank the staff of P04 at Petra III, and U41 PGM and UE52-SGM at BESSY for their continuous support. We thank W. Quevedo for his for his help during the beamtimes at BESSY.

M.O. acknowledges funding from the Swedish Research Council (VR contract 2021-04521). M.O. and A.B. acknowledge support from Carl Tryggers Foundation (contract CTS 18:285). The calculations were partially enabled by resources provided by the Swedish National Infrastructure for Computing (SNIC) at at the Swedish National Supercomputer Center (NSC), the High Performance Computer Center North (HPC2N), and Chalmers Centre for Computational Science and Engineering (C3SE) partially funded by the Swedish Re-

search Council through grant agreement no. 2018-05973. S.T. is grateful to the DFG for financial support of the project C04/SFB1633 "Proto-coupled electron transfer.

References

(1) Bandara, H. M. D.; Burdette, S. C. Photoisomerization in different classes of azobenzene. *Chem. Soc. Rev.* **2012**, *41*, 1809–1825.

(2) Tan, E. M. M.; Amirjalayer, S.; Smolarek, S.; Vdovin, A.; Zerbetto, F.; Buma, W. J. Fast photodynamics of azobenzene probed by scanning excited-state potential energy surfaces using slow spectroscopy. *Nat. Commun.* **2015**, *6*, 5860,1–7.

(3) Magee, J. L.; Shand, W.; Eyring, H. Non-adiabatic Reactions. Rotation about the Double Bond. *J. Am. Chem. Soc.* **1941**, *63*, 677–688.

(4) Schoenlein, R. W.; Peteanu, L. A.; Mathies, R. A.; Shank, C. V. The first step in vision: femtosecond isomerization of rhodopsin. *Science* **1991**, *254*, 412–415.

(5) Dugave, C.; Demange, L. Cis-trans isomerization of organic molecules and biomolecules: Implications and applications. *Chem. Rev.* **2003**, *103*, 2475–2532.

(6) Banghart, M.; Borges, K.; Isacoff, E.; Trauner, D.; Kramer, R. H. Light-activated ion channels for remote control of neuronal firing. *Nat. Neurosci.* **2004**, *7*, 1381–1386.

(7) Gruhl, T. et al. Ultrafast structural changes direct the first molecular events of vision. *Nature* **2023**, *615*, 939–944.

(8) Yin, H.; Chen, J.; Zheng, D. Effect of Molecular Substitution and Isomerization on Charge-Transport Parameters in Molecular Organic Semiconductors. *J. Phys. Chem. Lett.* **2021**, *12*, 2660–2667.

(9) Luo, S.; Zhao, Y.; Truhlar, D. G. Validation of electronic structure methods for isomerization reactions of large organic molecules. *Phys. Chem. Chem. Phys.* **2011**, *13*, 13683–13689.

(10) Muraoka, T.; Kinbara, K.; Aida, T. Mechanical twisting of a guest by a photoresponsive host. *Nature* **2006**, *440*, 512–515.

(11) Zhang, B.; Feng, Y.; Feng, W. Azobenzene-based solar thermal fuels: A review. *Nano Micro Lett.* **2022**, *14*, 138.

(12) Zimmerman, G.; Chow, L.-Y.; Paik, U.-J. The Photochemical Isomerization of Azobenzene. *J. Am. Chem. Soc.* **1958**, *80*, 3528–3531.

(13) Griffiths, J. II. Photochemistry of azobenzene and its derivatives. *Chem. Soc. Rev.* **1972**, *1*, 481–493.

(14) Forber, C. L.; Kelusky, E. C.; Bunce, N. J.; Zerner, M. C. Electronic Spectra of cis-and trans-Azobenzenes: Consequences of Ortho Substitution. *J. Am. Chem. Soc.* **1985**, *107*, 5884–5890.

(15) Rau, H.; Lüddecke, E. On the Rotation-Inversion Controversy on Photoisomerization of Azobenzenes. Experimental Proof of Inversion. *J. Am. Chem. Soc.* **1982**, *104*, 1616–1620.

(16) Barbatti, M.; Aquino, A. J.; Szymczak, J. J.; Nachtigallová, D.; Hobza, P.; Lischka, H. Relaxation mechanisms of UV-photoexcited DNA and RNA nucleobases. *Proc. Nat. Acad. Sci. U.S.A.* **2010**, *107*, 21453–21458.

(17) Horio, T.; Spesyvtsev, R.; Nagashima, K.; Ingle, R. A.; Suzuki, Y.-i.; Suzuki, T. Full observation of ultrafast cascaded radiationless transitions from S2 ($\pi\pi*$) state of pyrazine using vacuum ultraviolet photoelectron imaging. *J. Chem. Phys.* **2016**, *145*, 044306.

(18) Sun, K.; Xie, W.; Chen, L.; Domcke, W.; Gelin, M. F. Multi-faceted spectroscopic mapping of ultrafast nonadiabatic dynamics near conical intersections: A computational study. *J. Chem. Phys.* **2020**, *153*, 174111.

(19) Kowalewski, M.; Fingerhut, B. P.; Dorfman, K. E.; Bennett, K.; Mukamel, S. Simulating coherent multidimensional spectroscopy of nonadiabatic molecular processes: From the infrared to the x-ray regime. *Chem. Rev.* **2017**, *117*, 12165–12226.

(20) Stuart, C. M.; Frontiera, R. R.; Mathies, R. A. Excited-State Structure and Dynamics of cis- and trans-Azobenzene from Resonance Raman Intensity Analysis. *J. Phys. Chem. A* **2007**, *111*, 12072–12080.

(21) Nenov, A.; Borrego-Varillas, R.; Oriana, A.; Ganzer, L.; Segatta, F.; Conti, I.; Segarra-Marti, J.; Omachi, J.; Dapor, M.; Taioli, S.; Manzoni, C.; Mukamel, S.; Cerullo, G.; Garavelli, M. UV-Light-Induced Vibrational Coherences: The Key to Understand Kasha Rule Violation in trans -Azobenzene. *J. Phys. Chem. Lett.* **2018**, *9*, 1534–1541.

(22) Yu, J. K.; Bannwarth, C.; Liang, R.; Hohenstein, E. G.; Martínez, T. J. Nonadiabatic dynamics simulation of the wavelength-dependent photochemistry of azobenzene excited to the nπ^* and $\pi\pi^*$ excited states. *J. Am. Chem. Soc.* **2020**, *142*, 20680–20690.

(23) Otolski, C. J.; Raj, A. M.; Ramamurthy, V.; Elles, C. G. Spatial confinement alters the ultrafast photoisomerization dynamics of azobenzenes. *Chem. Sci.* **2020**, *11*, 9513–9523.

(24) Rouxel, J. R.; Keefer, D.; Aleotti, F.; Nenov, A.; Garavelli, M.; Mukamel, S. Coupled Electronic and Nuclear Motions during Azobenzene Photoisomerization Monitored by Ultrafast Electron Diffraction. *J. Chem. Theory Comput.* **2022**, *18*, 605–613.

(25) Ament, L. J. P.; van Veenendaal, M.; Devereaux, T. P.; Hill, J. P.; van den Brink, J. Resonant inelastic x-ray scattering studies of elementary excitations. *Rev. Mod. Phys.* **2011**, *83*, 705.

(26) Nordgren, J.; Rubensson, J.-E. Resonant soft X-ray emission for studies of molecules and solids. *J. Electron Spectrosc. Relat. Phenom.* **2013**, *188*, 3 – 9.

(27) Gel'mukhanov, F.; Odelius, M.; Polyutov, S. P.; Föhlisch, A.; Kimberg, V. Dynamics of resonant x-ray and auger scattering. *Rev. Mod. Phys.* **2021**, *93*, 035001.

(28) Gel'mukhanov, F.; Ågren, H. Resonant X-ray Raman scattering. *Phys. Rep.* **1999**, *312*, 87.

(29) Kunnus, K. et al. A setup for resonant inelastic soft x-ray scattering on liquids at free electron laser light sources. *Rev. Sci. Instrum.* **2012**, *83*, 123109.

(30) Yin, Z.; Peters, H.-B.; Hahn, U.; Gonschior, J.; Mierwaldt, D.; Rajkovic, I.; Viefhaus, J.; Jooss, C.; Techert, S. An endstation for resonant inelastic X-ray scattering studies of solid and liquid samples. *J. Synchrotron Radiat.* **2017**, *24*, 302–306.

(31) Agåker, M. et al. The 10 m collimated Rowland spectrometer at the MAX IV Veritas beamline. *Synchrotron Radiat.* **2025**, *32*, 1328—-1345.

(32) Ekimova, M.; Quevedo, W.; Faubel, M.; Wernet, P.; Nibbering, E. T. A liquid flatjet system for solution phase soft-x-ray spectroscopy. *Struc. Dyn.* **2015**, *2*, 014303, 1–7.

(33) Malerz, S.; Haak, H.; Trinter, F.; Stephansen, A. B.; Kolbeck, C.; Pohl, M.; Hergenhahn, U.; Meijer, G.; Winter, B. A setup for studies of photoelectron circular dichroism from chiral molecules in aqueous solution. *Rev. Sci. Instrum.* **2022**, *93*, 015101, 1–16.

(34) Kleine, C.; Ekimova, M.; Goldsztejn, G.; Raabe, S.; Strüber, C.; Ludwig, J.; Yarlagadda, S.; Eisebitt, S.; Vrakking, M. J. J.; Elsaesser, T.; Nibbering, E. T. J.; Rouzée, A. Soft X-ray absorption spectroscopy of aqueous solutions using a table-top femtosecond soft X-ray source. *J. Phys. Chem. Lett.* **2018**, *10*, 52–58.

(35) Yin, Z.; Chang, Y.-P.; Balčiūnas, T.; Shakya, Y.; Djorović, A.; Gaulier, G.; Fazio, G.;

Santra, R.; Inhester, L.; Wolf, J.-P.; Wörner, H. J. Femtosecond proton transfer in urea solutions probed by X-ray spectroscopy. *Nature* **2023**, *619*, 749–754.

(36) Schlappa, J. et al. The Heisenberg-RIXS instrument at the European XFEL. *Synchrotron Radiat.* **2025**, *32*, 29—-45.

(37) Carlini, L. et al. Electron and ion spectroscopy of azobenzene in the valence and core shells. *J. Chem. Phys.* **2023**, *158*, 054201, 1–15.

(38) Cocchi, C.; Draxl, C. Bound excitons and many-body effects in x-ray absorption spectra of azobenzene-functionalized self-assembled monolayers. *Phys. Rev. B* **2015**, *92*, 205105.

(39) Segatta, F.; Nenov, A.; Orlandi, S.; Arcioni, A.; Mukamel, S.; Garavelli, M. Exploring the capabilities of optical pump X-ray probe NEXAFS spectroscopy to track photo-induced dynamics mediated by conical intersections. *Faraday Discuss.* **2020**, *221*, 245–264.

(40) Hohenstein, E. G.; Yu, J. K.; Bannwarth, C.; List, N. H.; Paul, A. C.; Folkestad, S. D.; Koch, H.; Martinez, T. J. Predictions of pre-edge features in time-resolved near-edge X-ray absorption fine structure spectroscopy from hole–hole Tamm–Dancoff-Approximated density functional theory. *J. Chem. Theory Comput.* **2021**, *17*, 7120–7133.

(41) Schmidt, R.; Hagen, S.; Brete, D.; Carley, R.; Gahl, C.; Dokić, J.; Saalfrank, P.; Hecht, S.; Tegeder, P.; Weinelt, M. On the electronic and geometrical structure of the trans-and cis-isomer of tetra-tert-butyl-azobenzene on Au (111). *Phys. Chem. Chem. Phys.* **2010**, *12*, 4488–4497.

(42) Ulrich, S.; Jung, U.; Strunskus, T.; Schütt, C.; Bloedorn, A.; Lemke, S.; Ludwig, E.; Kipp, L.; Faupel, F.; Magnussen, O.; Herges, R. X-ray spectroscopy characterization

of azobenzene-functionalized triazatriangulenium adlayers on Au (111) surfaces. *Phys. Chem. Chem. Phys.* **2015**, *17*, 17053–17062.

(43) Engel, R. Y. et al. Shot noise limited soft x-ray absorption spectroscopy in solution at a SASE-FEL using a transmission grating beam splitter. *Struc. Dyn.* **2021**, *8*, 014303, 1–7.

(44) Tomasi, J.; Mennucci, B.; Cammi, R. Quantum mechanical continuum solvation models. *Chem. Rev.* **2005**, *105*, 2999–3094.

(45) Zhao, Y.; Truhlar, D. G. The M06 suite of density functionals for main group thermochemistry, thermochemical kinetics, noncovalent interactions, excited states, and transition elements: two new functionals and systematic testing of four M06-class functionals and 12 other functionals. *Theor. Chem. Acc.* **2008**, *120*, 215–241.

(46) Weigend, F.; Ahlrichs, R. Balanced basis sets of split valence, triple zeta valence and quadruple zeta valence quality for H to Rn: Design and assessment of accuracy. *Phys. Chem. Chem. Phys.* **2005**, *7*, 3297–3305.

(47) Riley, K. E.; Pitonak, M.; Cerny, J.; Hobza, P. On the Structure and Geometry of Biomolecular Binding Motifs (Hydrogen-Bonding, Stacking, X–H $\cdots\pi$): WFT and DFT Calculations. *J. Chem. Theory Comput.* **2010**, *6*, 66–80, PMID: 26614320.

(48) Frisch, M. J. et al. Gaussian˜16 Revision C.01. 2016; Gaussian Inc. Wallingford CT.

(49) da Cruz, V. V.; Eckert, S.; Föhlisch, A. TD-DFT simulations of K-edge resonant inelastic X-ray scattering within the restricted subspace approximation. *Phys. Chem. Chem. Phys.* **2021**, *23*, 1835–1848.

(50) Neese, F. The ORCA program system. *Wiley Interdisc. Rev. - Comput. Mol. Sci.* **2012**, *2*, 73–78.

(51) Yanai, T.; Tew, D. P.; Handy, N. C. A new hybrid exchange–correlation functional using the Coulomb-attenuating method (CAM-B3LYP). *Chem. Phys. Lett.* **2004**, *393*, 51–57.

(52) Jacquemin, D.; Preat, J.; Perpète, E. A.; Vercauteren, D. P.; André, J.-M.; Ciofini, I.; Adamo, C. Absorption spectra of azobenzenes simulated with time-dependent density functional theory. *Internat. J. Quant. Chem.* **2011**, *111*, 4224–4240.

(53) Lu, T.; Chen, F. Multiwfn: A multifunctional wavefunction analyzer. *J. Comput. Chem.* **2012**, *33*, 580–592.

(54) Gel'mukhanov, F.; Ågren, H. Resonant inelastic x-ray scattering with symmetry-selective excitation. *Phys. Rev. A* **1994**, *49*, 4378–4389.

(55) Norman, P.; Dreuw, A. Simulating X-ray spectroscopies and calculating core-excited states of molecules. *Chem. Rev.* **2018**, *118*, 7208–7248.

(56) Hennies, F.; Pietzsch, A.; Berglund, M.; Föhlisch, A.; Schmitt, T.; Strocov, V.; Karlsson, H. O.; Andersson, J.; Rubensson, J.-E. Resonant inelastic scattering spectra of free molecules with vibrational resolution. *Phys. Rev. Lett.* **2010**, *104*, 193002.

(57) Pietzsch, A.; Niskanen, J.; da Cruz, V. V.; Büchner, R.; Eckert, S.; Fondell, M.; Jay, R. M.; Lu, X.; McNally, D.; Schmitt, T.; Föhlisch, A. Cuts through the manifold of molecular H2O potential energy surfaces in liquid water at ambient conditions. *Proc. Nat. Acad. Sci. U.S.A.* **2022**, *119*, e2118101119.

(58) Rau, H. *Photochemistry and photophysics*; CRC Press: Boca Raton, FL, 1989; Vol. 1; Chapter 4, pp 119–141.

(59) Keefer, D.; Aleotti, F.; Rouxel, J. R.; Segatta, F.; Gu, B.; Nenov, A.; Garavelli, M.; Mukamel, S. Imaging conical intersection dynamics during azobenzene photoisomerization by ultrafast X-ray diffraction. *Proc. Nat. Acad. Sci. U.S.A.* **2021**, *118*, 1–10.

(60) Gu, B.; Keefer, D.; Aleotti, F.; Nenov, A.; Garavelli, M.; Mukamel, S. Photoisomerization transition state manipulation by entangled two-photon absorption. *Proc. Nat. Acad. Sci. U.S.A.* **2021**, *118*, e2116868118.

(61) Wang, C.; Kimberg, V.; Gong, M.; Cheng, Y.; Liu, X.-J.; Vendrell, O.; Ueda, K.; Zhang, S. B. Tracking conical intersection passage with time-resolved resonant Auger scattering. *Phys. Rev. A* **2024**, *110*, 042811, 1–13.

(62) Fregoni, J.; Granucci, G.; Coccia, E.; Persico, M.; Corni, S. Manipulating azobenzene photoisomerization through strong light–molecule coupling. *Nature commun.* **2018**, *9*, 4688.